Fusion Journal of Engineering and Sciences

Research Article

Numerical Investigation of Hybrid Fiber Reinforced Concrete (HyFRC) Bridge Pier for Seismic Prone Area

Asad Ullah [1], Qaiser uz Zaman Khan[1], Aftab Khan[1], Areej Ahmed [1] and Tufail Mabood [2,*]

[1] University of Engineering and Technology, Taxila; engr.asadullah138@gmail.com, dr.qaiser@uettaxila.edu.pk; aftabkhanengineer@gmail.com; engrareejahmed@gmail.com
[2] University of Engineering and Technology, Peshawar; 13bnciv0557@gmail.com
* Correspondence: engr.asadullah138@gmail.com; Tel.: +92302 5515191

Abstract

Bridge Piers are critical structural elements that govern the stability and seismic performance of bridges where enhanced ductility is essential to prevent failure under strong seismic loadings. The current research work investigates the experimental findings of Hybrid Fiber Reinforced Concrete (HyFRC) bridge pier, in a seismic-prone area followed by numerical simulation. Three circular scaled-down bridge piers: one conventional control and two HyFRC specimens integrated with 0.25% steel and 0.2% polypropylene fibers by weight of cement were tested under a quasi-static cyclic loading up to 4% drift and a constant axial load of 20 tons. A non-linear finite element analysis (NLFEA) model was developed in ABAQUS, utilizing a user-defined subroutine material (UMAT). The NLFEA model accurately reflected the reinforcement configuration, geometric dimensions and boundary conditions consistent with the experimental setup to capture the complex behavior. The seismic performance of piers was investigated by comparing different parameters, including hysteresis-based parameters, energy dissipation, and visual damage patterns. The results obtained from the numerical model showed strong correlation with experimental results, highlighting the model's ability to capture the non-linear behavior of the pier under seismic loading. These findings show that the model can accurately predict the seismic performance of HyFRC bridge piers, supporting the design of bridges with enhanced resistance to earthquake loading.

Keywords: Hybrid Fiber Reinforced Concrete (HyFRC), Nonlinear Finite Element Analysis (NLFEA), User-Defined Material Subroutine (UMAT), seismic performance, experimental validation

1. Introduction

Bridge piers are the most critical components of highway and railway bridges in earthquake-prone regions [1, 2]. When a strong ground motion hits, they must absorb and dissipate huge amounts of energy while keeping the superstructure stable [3, 4]. Historical earthquakes have repeatedly shown that ordinary reinforced concrete piers often fail in a brittle manner through concrete crushing, cover spalling, buckling of longitudinal bars, and sudden loss of lateral strength [5–9]. Such failures lead to collapse or extremely expensive retrofitting. Therefore, improving the ductility, energy dissipation capacity,

and damage tolerance of bridge piers has become a major research and practical priority worldwide [10–12].

One of the most effective and practical ways to achieve this improvement is by adding discrete fibers into the concrete mix [13–15]. Steel fibers increase the peak load and control crack propagation at small and moderate deformations, whereas macro-synthetic (polypropylene) fibers continue to bridge cracks even at very large openings, providing a long and stable softening branch [16, 17]. When both types are combined at low dosage, the resulting hybrid fiber-reinforced concrete (HyFRD) shows remarkable synergy: the concrete becomes much tougher in tension, cracks remain fine and well-distributed, spalling is delayed or eliminated, and the overall seismic behavior becomes far more ductile than conventional reinforced concrete [18, 19].

Although many studies have already proved the advantages of HyFRD in beams, columns, and shear walls, very few experimental programs have focused on realistic bridge piers subjected to constant axial load and reversed cyclic lateral displacement [20]. Even fewer have proposed simple, engineer-friendly numerical models that can directly use standard material test results (compressive strength, modulus, splitting tensile strength, and fracture energy) without complicated micro-modelling of individual fibers or special interface elements [21–23].

The present study addresses this gap by testing three 1/4-scale circular bridge piers under quasi-static cyclic loading and constant axial compression. The first pier of 18 MPa was made of conventional reinforced concrete and served as the control specimen. The second piers were cast using low-dosage HyFRD mixtures containing only 0.25 % hooked-end steel fibers by weight of cement, with target matrix strengths of 22 MPa, respectively. The experimental program aimed to quantify the improvement in lateral strength, hysteretic behavior, energy dissipation, damping, and ultimate drift capacity brought by the hybrid fibers.

To enable practical application of the findings, a straightforward continuum damage model (Mazars model implemented as an ABAQUS user-material subroutine) was calibrated exclusively from cylinder and fracture energy tests. The effect of discrete fibers was modelled, and parameters were adjusted on the pier response itself. The validated numerical platform demonstrates that the beneficial macroscopic effects of low-dosage hybrid fibers can be reliably and simply captured through properly measured tensile fracture energy and residual tensile capacity, offering practicing engineers an efficient tool for performance-based seismic design and assessment of HyFRD bridge piers.

2. Materials and Methods

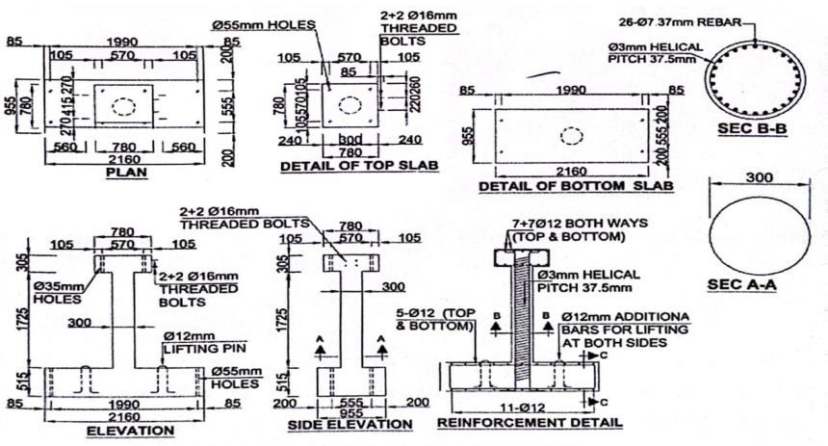

Figure 1: Geometry and reinforcement details of the 1/4-scale circular bridge pier specimens (all dimensions in mm

The experimental program comprised two identical 1/4-scale circular bridge piers tested under quasi-static reversed cyclic loading: one conventional reinforced concrete pier (referred to as Control) and one hybrid fiber-reinforced concrete pier (referred to as Model 1). Both piers were designed to represent typical medium-span highway bridge piers in moderate-seismicity regions of Pakistan, where concrete compressive strength is usually in the range of 18–25 MPa and axial load ratio remains low to moderate. The geometry and reinforcement details of the tested bridge piers are shown in **Error! Reference source not found.**.

The concrete mixture for the Control specimen was a standard mix using locally used in bridge construction: Ordinary Portland cement (Fauji Cement), natural river sand (fineness modulus 2.52), and 20 mm down crushed limestone aggregate. The target 28-day cylinder compressive strength was 18 MPa, and no fibers were added. For Model 1 used the same base materials and cement content but incorporated a low-dosage hybrid fiber combination: 0.25 % (by weight of cement) copper-coated hooked-end steel fibers (diameter 0.56 mm, length 30 mm, tensile strength 2850 MPa) and 0.20 % macro-polypropylene fibers (equivalent diameter 0.8–1.8 mm, length 48 mm, tensile strength 300–400 MPa). The water-cement ratio was kept almost identical to maintain comparable workability (slump ≈ 80 mm). Achieved 28-day cylinder strengths were 22 MPa for the Model 1 and 18 MPa for Control Model, while splitting tensile strength jumped from 2.1 MPa to 3.17 MPa due to the fibers.

Both piers had an external diameter and a clear height from the top of the stiff foundation block to the centerline of the lateral loading actuator. Longitudinal reinforcement and transverse reinforcement were provided as per the specifications provided in **Error! Reference source not found.**. Grade 60 steel (yield strength 460 MPa) was used for all bars. The foundation block was heavily reinforced and post-tensioned to the strong floor to prevent any uplift or sliding during testing. The finished specimens ready for testing are shown in **Figure 2**. (**a**) View of the two 1/4-scale bridge pier specimens prior to testing; (**b**) View of the 1/4-scale bridge pier specimens during testing.Both piers had an identical external appearance and geometry. The only difference was the addition of low-dosage hybrid steel and macro-polypropylene fibers in Model 1, which were uniformly distributed throughout the concrete volume during mixing and are not visible on the surface.

(**a**) (**b**)

Figure 2. (**a**) View of the two 1/4-scale bridge pier specimens prior to testing; (**b**) View of the 1/4-scale bridge pier specimens during testing.

Testing was carried out on a hydraulic testing frame at the Earthquake Engineering Center, UET Peshawar. A constant axial load of 196 kN (approximately 10 % of the gross concrete axial capacity) was applied at the top through modular slabs and maintained within ±3 % during the entire test. Lateral displacement was imposed following the **Error! Reference source not found.** protocol. Lateral load, displacement, axial load, and strains in longitudinal and spiral reinforcement were continuously recorded at each data point. Three-dimensional nonlinear finite element models of both piers were developed in ABAQUS/Standard 2016 using the same geometry and reinforcement as the tested specimens. Concrete was modelled with 8-node linear brick elements with reduced integration (C3D8R), while all reinforcing bars were modelled as 2-node linear 3D truss elements (T3D2) using Grade-60 steel properties (fy = 460 MPa, E = 200 GPa, elastic-perfectly plastic). Reinforcement was embedded in concrete using the embedded region constraint. The 196 kN constant axial load was applied on top face of the upper face of bridge pier, while reversed-cyclic lateral displacement was imposed on the coupled reference point using the exact experimental displacement history (refer to **Figure 3**).

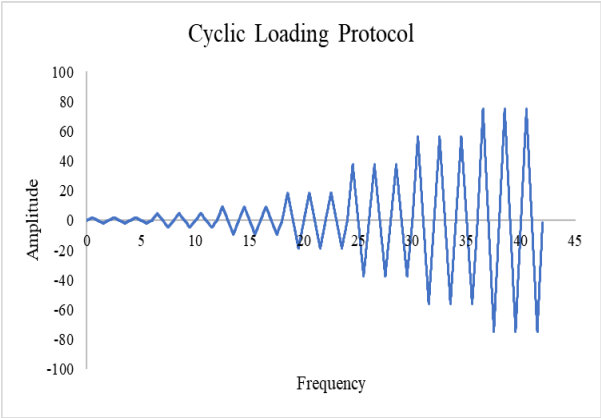

Figure 3: Cyclic Loading Protocol Adopted in both Experimental and Numerical Study

A mesh sensitivity study was performed; a global seed size of 25 mm in the pier and 25 mm in the top/bottom pads provided the best balance between accuracy and computational cost and was therefore adopted for all analyses (total elements 10977 for both Models). Concrete behavior was defined using the Mazars scalar damage model implemented through a user-material subroutine (UMAT); all parameters were taken directly from the material tests with no adjustment on the pier response. Two static-general steps were defined after the initial step: (1) application of axial load, and (2) cyclic lateral displacement. Jobs were created and submitted automatically via Python scripting.

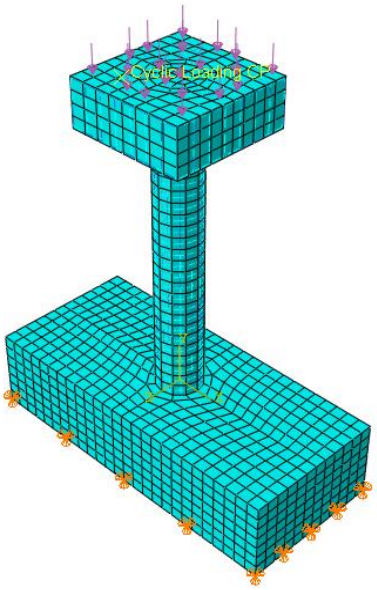

Figure 4: Finite element model of the tested bridge pier in ABAQUS

3. Results

The Control specimen (plain reinforced concrete) experienced classic flexural failure at the pier–foundation interface (refer to **Figure 4**). At approximately 4.8 % drift, wide horizontal cracks opened at the base, followed by extensive cover spalling, exposure of the spiral reinforcement, and subsequent buckling of the longitudinal bars, leading to a sudden drop in lateral resistance. The numerical model accurately captured this behavior: the tensile damage variable (SDV2) from the Mazars UMAT, correctly predicting both the location and the severity of crushing and spalling. In contrast, Model 1 (hybrid fiber-reinforced concrete) showed no visible spalling or bar buckling even after reaching 7 % drift (refer to **Figure 4**). Instead, only numerous fine, closely spaced hairline cracks were distributed over the lower 500 mm of the pier, confirming the effectiveness of the low-dosage hybrid fibers in bridging cracks and preserving concrete integrity. The corresponding numerical simulation reflected this superior performance: the tensile damage variable remained well-distributed and significantly lower in magnitude, with no localized high-damage zone at the base, demonstrating that the calibrated Mazars model reliably reproduces the transition from concentrated damage in plain concrete to diffuse micro-cracking in HyFRD without any special fibre elements.

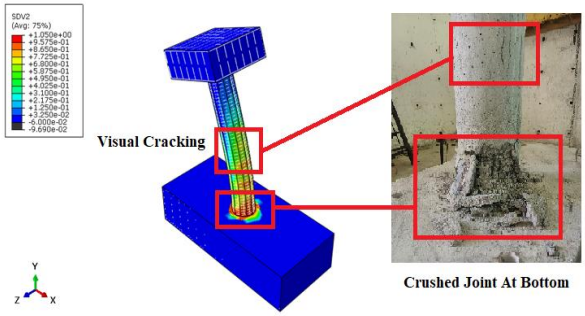

Figure 5: Comparison of observed and predicted damage at failure for the Control specimen (Model-1)

The experimental backbone curves for both piers are presented in **Figure 5** & **Figure 6**, constructed by connecting the peak load of the first cycle at each imposed drift level in positive (push) and negative (pull) directions separately. For the Control specimen (plain RC)

pier, the positive-direction backbone reached a maximum lateral load of 25.8 kN at approximately 20 mm displacement, while the negative direction peaked at only 21.8 kN at the same drift level, revealing clear asymmetry (negative strength is less than that of the positive). After the peak, strength degraded rapidly: at 60 mm the positive load had dropped to 19.6 kN and the negative load to 16.8 kN (average retained capacity is less than that of respective peaks). By so much drift the pier had suffered cover spalling and longitudinal bar buckling, resulting in a residual capacity of approximately 18 kN in both directions.

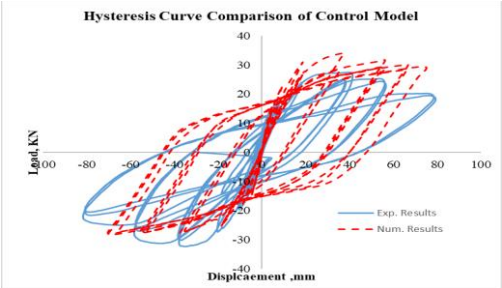

Figure 6: Hysteresis Curve Comparison of Control Model

In sharp contrast, Model 1 (HyFRD pier) exhibited almost perfect symmetry throughout the test. The positive backbone peaked at 30.6 kN at 20 mm displacement, while the negative backbone reached 29.9 kN at the same drift level (negative strength is equal to approximate of positive). More importantly, the post-peak behaviour was dramatically improved: at 40 mm, the pier still carried 28.4 kN (positive) and 27.8 kN (negative), corresponding to the respective peak values. Even at the final drift of 60 mm, the sustained loads remained 28.1 kN (positive) and 27.5 kN (negative) with virtually no strength degradation and no visible spalling or bar buckling.

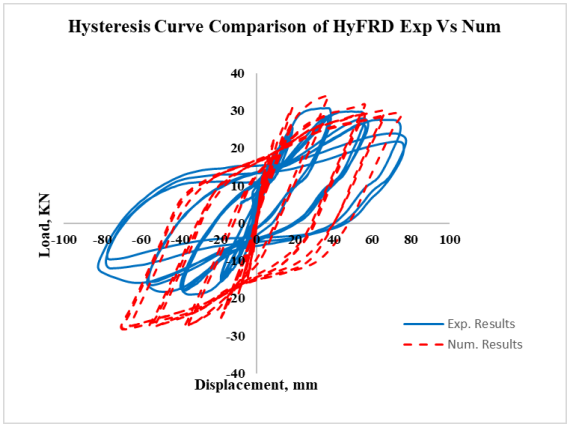

Figure 7: Hysteresis Curve Comparison of HyFRD Experimental Vs Numerical Models

These backbone curves unequivocally demonstrate that incorporating only a minor amount by weight of cement inclusion of hybrid steel + macro-polypropylene fibers increased the peak lateral, shifted the drift at peak strength, and – most crucially – transformed a steeply descending post-peak branch into an almost flat plateau that retained of peak capacity beyond 60 mm displacement. Such sustained load-carrying ability at extreme deformations is rarely achieved in conventional reinforced concrete piers and confirms the outstanding efficiency of low-dosage hybrid fiber reinforcement for seismic applications.

5. Conclusions

The quasi-static reversed-cyclic tests on two identical 1/4-scale circular bridge piers – one conventional reinforced concrete (Control) and one with only 0.45 % total hybrid fibers added to an ordinary 18 MPa concrete matrix – lead to the following clear conclusions:

Low-dosage hybrid fiber reinforcement dramatically enhances every key aspect of seismic performance. Despite lower concrete compressive strength, the HyFRD pier (Model 1) achieved higher peak lateral strength, higher initial stiffness, and higher cumulative energy dissipation than the plain RC pier. More importantly, it exhibited nearly perfect symmetry, virtually no pinching, and retained its peak load at 7 % drift, whereas the Control pier retained only 74 % and failed by bar buckling and spalling.

The failure mode was completely transformed. The Control pier suffered classic brittle-to-ductile transition failure with wide concentrated cracks, extensive cover spalling, and longitudinal bar buckling. Model 1 developed hundreds of fine, closely spaced cracks distributed over the lower portion, showed no spalling whatsoever, and kept all longitudinal bars perfectly straight up to the end of testing, demonstrating exceptional damage tolerance and residual load-carrying capacity.

The Mazars scalar damage model, implemented as an ABAQUS UMAT and calibrated exclusively from standard material tests, accurately reproduced the entire cyclic response of both piers without any inverse fitting at the component level and without modelling individual fibers. Errors on peak load, initial stiffness, and cumulative dissipated energy remained for both specimens, confirming that the macroscopic benefits of low-dosage hybrid fibers can be reliably and simply captured through enhanced tensile fracture energy and a modest residual tensile stress ratio.

6. Recommendations for Practice and Future Research

Based on the extensive research performed in this study, it is recommended that:

Low-dosage hybrid steel + macro-polypropylene fiber reinforcement (total dosage ≤ 0.5 % by weight of cement) is strongly recommended as a simple, robust, and cost-effective seismic enhancement technique for new and existing bridge piers in moderate-to-high seismicity regions, especially when high-strength or heavily confined concrete is not feasible.

The proposed Mazars UMAT modelling approach, using only standard material test data, offers practising engineers an efficient and sufficiently accurate tool for performance-based design and nonlinear dynamic analysis of HyFRD bridge piers without the complexity of discrete fiber or embedded-element modelling.

Further full-scale tests and long-term durability studies are recommended to confirm the observed benefits under real bridge axial load ratios and to establish practical design guidelines and code provisions for hybrid fiber-reinforced concrete bridge piers.

These findings demonstrate that a minor and inexpensive modification of the concrete mix can turn an ordinary bridge pier into a highly ductile, energy-dissipating, and damage-tolerant structural element capable of withstanding extreme seismic demands with minimal repair needs.

Abbreviations

The following abbreviations are used in this manuscript:

RC	Reinforced Concrete
HyFRC	Hybrid Fiber-Reinforced Concrete
HyFRD	Hybrid Fiber-Reinforced Concrete
f′c, fcm	Cylinder compressive strength of concrete

fctm	Mean tensile strength of concrete (from splitting test)
Gf,I	Mode-I (tensile) fracture energy
Gf,II or GfIc	Mode-II (compressive) fracture energy (= 100 × Gf,I)
ϱl	Longitudinal reinforcement ratio
ϱv	Volumetric transverse (spiral) reinforcement ratio
UMAT	User-defined material subroutine in ABAQUS
SDV2	State-dependent variable 2 (tensile damage parameter Dt in Mazars model)
C3D8R	8-node linear brick element with reduced integration in ABAQUS
T3D2 2-	node linear 3D truss element in ABAQUS

References

[1] M. J. N. Priestley and G. M. Calvi, "Strategies for repair and seismic upgrading of bolu viaduct 1, Turkey," *J Earth Eng*, vol. 06, no. spec01, pp. 157–184, 2002, doi: 10.1142/s1363246902000681.

[2] S. Motaref, M. S. Saiidi, and D. Sanders, "Shake table studies of energy-dissipating segmental bridge columns," *J Bridg. Eng.*, vol. 19, no. 2, pp. 186–199, Feb. 2014, doi: 10.1061/(asce)be.1943-5592.0000518.

[3] J. B. K. Pang, M. O. Eberhard, and J. F. Stanton, "Large-bar connection for precast bridge bents in seismic regions," *J Bridg. Eng.*, vol. 15, no. 3, pp. 231–239, May 2010, doi: 10.1061/(asce)be.1943-5592.0000081.

[4] B. Khaleghi *et al.*, "Accelerated bridge construction in Washington State: from research to practice," *pcij*, vol. 57, no. 4, pp. 34–49, 2012, doi: 10.15554/pcij.09012012.34.49.

[5] M. Mehraein and S. Saiidi, "Seismic performance and design of bridge column-to-pile shaft pipe-pin connections in precast and cast-in-place bridges," *Earthq Eng Struct Dyn.*, vol. 48, no. 13, pp. 1471–1490, Oct. 2019, doi: 10.1002/eqe.3209.

[6] Y.-C. Ou, M. Chiewanichakorn, A. J. Aref, and G. C. Lee, "Seismic performance of segmental precast unbonded post-tensioned concrete bridge columns," *J Struc Eng NY*, vol. 133, no. 11, p. 1636, Nov. 2007, doi: 10.1061/(asce)0733-9445(2007)133:11(1636).

[7] E. L. Yang, G. Liang, B. Rajlic, and P. Murray, "Hodder Avenue underpass: an innovative bridge solution with ultra-high performance fibre-reinforced concrete," *KEM*, vol. 629–630, pp. 37–42, 2014, doi: 10.4028/www.scientific.net/kem.629-630.37.

[8] M. Kenarkoohi and M. Hassan, "Review of accelerated construction of bridge piers - methods and performance," *Adv. Bridg. Eng. 2024 51*, vol. 5, no. 1, pp. 3-, Feb. 2024, doi: 10.1186/S43251-024-00116-6.

[9] A. Palermo and M. Mashal, "Accelerated Bridge construction (ABC) and seismic damage resistant technology: a New Zealand challenge," *Bull New Z Soc Earthq Eng*, vol. 45, no. 3, pp. 123–134, 2012, doi: 10.5459/bnzsee.45.3.123-134.

[10]M. Nader, "Accelerated bridge construction of the new samuel de champlain bridge," *J Bridg. Eng.*, vol. 25, no. 2, p. 05019015, Feb. 2020, doi: 10.1061/(asce)be.1943-5592.0001515.

[11]Z. H. Zong *et al.*, "Review on Anti-blast Resistance and Safety Protection of Bridge Structures," *Zhongguo Gonglu Xuebao/China J. Highw. Transp.*, vol. 37, no. 5, pp. 1–37, May 2024, doi: 10.19721/J.CNKI.1001-7372.2024.05.001.

[12]S. Harzallah, M. Chabaat, M. Saidani, and M. Moussaoui, "Numerical investigation of the seismic vulnerability of bridge piers strengthened with steel fibre reinforced concrete (SFRC) and carbon fibre composites (CFC)," *Case Stud. Constr. Mater.*, vol. 17, Dec. 2022, doi: 10.1016/J.CSCM.2022.E01235.

[13]C. Stratford, A. Palermo, and A. Scott, "Seismic Behavior of Concrete Bridge Piers Reinforced with Steel or GFRP Bars," *J. Compos. Constr.*, vol. 27, no. 2, Apr. 2023, doi: 10.1061/JCCOF2.CCENG-3945.

[14]G. Guerrini, A. Bruggi, S. Urso, M. Quaini, and A. Penna, "Cyclic shear-compression tests on two stone masonry piers strengthened with CRM and FRCM," *Procedia Struct. Integr.*, vol. 44, pp. 2214–2221, 2022, doi: 10.1016/J.PROSTR.2023.01.283.

[15]B. Piscesa, M. M. Attard, A. K. Samani, and S. Tangaramvong, "Plasticity constitutive model for stress-strain relationship of confined concrete," *ACI Mater. J.*, vol. 114, no. 2, pp. 361–371, Mar. 2017, doi: 10.14359/51689428.

[16]I. A. Sharaky, A. S. Elamary, and Y. M. Alharthi, "Experimental and numerical investigation on the flexural performance of RC slabs strengthened with EB/NSM CFRP reinforcement and bonded reinforced HSC layers," *Eng. Struct.*, vol. 289, Aug. 2023, doi: 10.1016/J.ENGSTRUCT.2023.116338.

[17]Q. H. Li and Y. Y. Zhang, "Dynamic response of SRP-reinforced precast segmental bridge columns subjected to vehicle collision," *Zhendong Gongcheng Xuebao/Journal Vib. Eng.*, vol. 34, no. 5, pp. 959–968, Oct. 2021, doi: 10.16385/J.CNKI.ISSN.1004-4523.2021.05.009.

[18]H. Naderpour and M. Mirrashid, "Evaluation and verification of finite element analytical models in reinforced concrete members," *Iran. J. Sci. Technol. Trans. Civ. Eng.*, vol. 44, no. 2, pp. 463–480, Jun. 2020, doi: 10.1007/s40996-019-00240-8.

[19]P. Poorahad Anzabi and M. R. Shiravand, "Segments Arrangement Effect on Improvement of Self-Centering Precast Post-Tensioned Segmental Piers Seismic Performance," *Struct. Concr.*, vol. 25, no. 1, pp. 185–206, Feb. 2024, doi: 10.1002/suco.202300133.

[20]S. Aldabagh, F. Hossain, and M. S. Alam, "Simplified Predictive Expressions of Drift Limit States for Reinforced Concrete Circular Bridge Columns," *J. Struct. Eng.*, vol. 148, no. 3, p. 04021285, Mar. 2022, doi: 10.1061/(asce)st.1943-541x.0003270.

[21]J. Zhang, J. Wu, Y. Qian, and Z. Guan, "Seismic behavior of prefabricated, assembled, self-centering bridge piers with a damage transfer configuration," *Earthq. Eng. Eng. Vib. 2025 243*, vol. 24, no. 3, pp. 861–874, Jul. 2025, doi: 10.1007/S11803-025-2341-5.

[22]N. Eini, S. M. Bateni, C. Jun, E. Heggy, and S. S. Band, "Estimation and interpretation of equilibrium scour depth around circular bridge piers by using optimized XGBoost and SHAP," *Eng. Appl. Comput. Fluid Mech.*, vol. 17, no. 1, 2023, doi: 10.1080/19942060.2023.2244558.

[23]A. H. M. M. Billah and A. Iqbal, "Effect of Seismic Isolation on Fragility of Bridges with Scoured Foundations," *J. Struct. Eng.*, vol. 148, no. 6, Jun. 2022, doi: 10.1061/(ASCE)ST.1943-541X.0003370.